X-ray Luminescent Properties of Zinc Oxide Films on the Sapphire M and A-Plane

© *I.D. Venevtsev* [1], *A.E. Muslimov* [2], *A.P. Tarasov* [2], *L.L. Emiraslanova* [3], *A.M. Ismailov* [3],
V.M. Kanevsky [2]

[1] Peter the Great Saint-Petersburg Polytechnic University, St. Petersburg, Russia
[2] Shubnikov Institute of Crystallography FSRC „Crystallography and Photonics" Russian Academy of Sciences, Moscow, Russia
[3] Dagestan State University, Makhachkala, Dagestan Republic, Russia
e-mail: Venevtsev.Ivan@gmail.com

The results of comparative studies of the processes of high-temperature synthesis, luminescence and scintillation characteristics of ZnO films on M(100)- and A(110)-orientation sapphire substrates are presented. It is shown that the use of the magnetron deposition method makes it possible to form, against the background of a continuous film, ensembles of individual [001] ZnO microcrystals with pronounced X-ray luminescent properties. The X-ray luminescence kinetics is characterized by two components: a fast component with a decay time in the order of a nanosecond and a slow luminescence component. The study of the films by photoluminescence spectroscopy revealed the features of the near-band-edge luminescence spectra of the samples, in particular, the presence of various excitonic emission channels. Differences in the spectral parameters of the near-band-edge luminescence band in the case of optical and X-ray excitation are found and interpreted.

Keywords: Films, microcrystals, zinc oxide, X-ray luminescence, photoluminescence, excitonic emission.

Introduction

Radiation-resistant scintillation materials based on oxides can be used as promising detectors of different radiation types. From the point of view of primary components availability and achievement of high scintillation characteristics of detector the ZnO-based structures are often considered as the most promising [1,2]. ZnO is characterized by the presence of edge ($380-400$ nm, with a typical deexcitation time of less than 1 ns [3]) and green defect (maximum in the region of $450-650$ nm, typical deexcitation time is about 1μs [4]) components of luminescence. Due to the absence of commercially available technology to manufacture single-crystals of ZnO [5,6], the most interesting today are ceramics, film technologies, ensembles of micro- and nano- crystals with different morphology. In our recent study [7] we have presented results of investigation of optical and luminescence properties of ZnO-based materials with different microstructure and morphology. The best scintillation characteristics (decay kinetics less than 1 ns) were demonstrated by gallium-doped ZnO ceramic and ensembles of nano- and micro- structures of ZnO. At the same time the ZnO ceramic materials demonstrated the highest transparency ($> 50\%$) at a thickness of 0.5 mm.

One of the key tasks related to the use of ZnO in scintillation detectors is the resolution enhancement. The scintillator resolution decreases dramatically at low optical homogeneity and uniformity of the material, its high grain boundary surface. Ensembles of ZnO microcrystals are not good in terms of uniformity and transparency. Among other factors, the resolution enhancement of single-crystal or ceramic ZnO scintillators can be achieved by reducing the sample thickness down to a few tens of micrometers, however it is difficult to implement from the technological point of view. In this context, very promising are ZnO films with a thickness of up to a few tens of micrometers with high crystal quality. The use of such films has the advantage of the technological possibility of applying the film directly onto the photodetector, as well as the high degree of transparency for the self-radiation. The limiting factor for the mass use of ZnO films is their low growth rate. The method of „uncooled target" with a growth rate increased up to 16 nm/s used in [8,9] has not allowed producing the required result: the films were growing with defects, with prevailing green luminescence (GL) in their X-ray luminescence (XRL) spectra. Recrystallization annealing in the air at a temperature of $1000°$C for 10 h only resulted in a greater GL due to the generation of additional number of oxygen vacancies.

It is known that the (001) plane in the crystal structure of ZnO has the lowest surface energy [10]. Thanks to this, the technology of manufacturing ZnO-based transparent electrodes in the form of dense arrays of [001]-oriented ZnO crystallites has become commonly used [11]. Usually the transparent electrodes are formed at low temperatures, and there is no practical need to grow film with a thickness greater than a few micrometers. For the high sensitivity of X-ray detector, a minimum thickness of the scintillator layer of a few tens of micrometers is necessary. With the use of
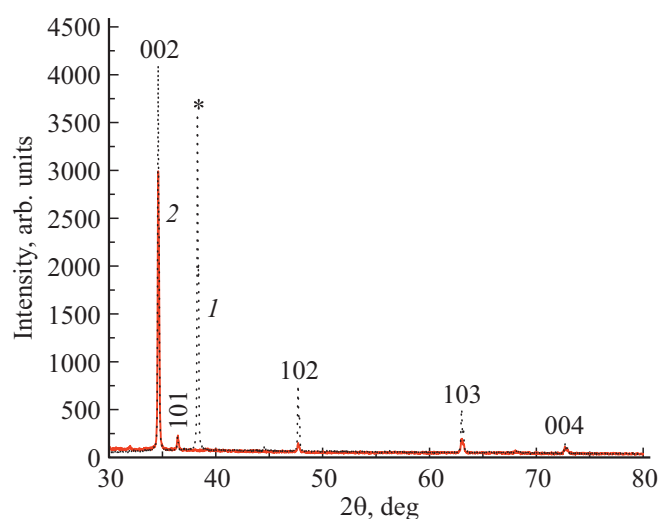
Figure 1. Patterns of XRD samples of ZnO films on A-type sapphire (curve *1*) and M-type (curve *2*). Legend: * — sapphire. JCPDS: 043-0002.

standard technology of applying transparent electrodes the resulted films are highly defective and peel off the substrate as they grow. It is suggested to address the problem of ZnO film peeling off with keeping the high growth rate and crystal quality through the use of high-temperature synthesis on sapphire substrates of non-basis orientation. The following was noted in the process of growth of ZnO films with polar and semipolar orientations: [100]-, [110]-, [103]- oriented epitaxial films of ZnO are transformed to [001]-textured films as they grow. Due to the structural-geometric conformity of lattices at the interphase boundary in the process of ZnO films growth on A- and M- plane sapphire, the following orientation relationships are implemented: (001)-ZnO‖ (110)-Al_2O_3 [12], (103)-ZnO‖ (100)-Al_2O_3 [13]. From the scientific and technological point of views of a great interest are the evolution of structure in the process of „thick" ZnO films synthesis and its effect on the growth rate and properties. This work presents the results of comparative studies of the processes of high-temperature synthesis, luminescence and scintillation characteristics of „thick" ZnO films on M(100)- and A(110)-orientation sapphire substrates are presented.

Materials and methods

Plates of M- and A- orientation sapphire were treated by the chemical-mechanical method. ZnO films (hereinafter referred to as M-type and A-type) were applied onto the surface of plates using the conventional „cooled" target in „VATT AMK-MI" („FerriVatt"LLC, Kazan) automated magnetron setup. Before each sputtering the vacuum chamber was pump out to a residual pressure of $\sim 9 \cdot 10^{-5}$ Pa. The working gas (oxygen) pressure was controlled by RRG-10 („Eltochpribor"LLC, Russia) and measured by TELEVAC CC-10 wide range vacuum gauge (USA). The

temperature of substrate was $750°$C. The substrate was heated by a resistive heater (nichrome). Depositing time was 2 h. In order to relax microstresses and improve crystal quality, the samples were postgrowth annealed in the open air at $800°$C for 2 h.

X-ray diffraction (XRD) studies were conducted using X'PERT PRO (PANalytical, the Netherlands) diffractometer in the Bragg−Brentano „ reflection" geometry with CuK_α radiation ($\lambda = 1.5418$ Å) with the use of Niβ-filter. Microscopic studies were conducted using Jeol Neoscope 2 (JCM-6000) scanning electron microscope. Film thicknesses were determined by investigating transverse sections of films using the electron microscopy method.

XRL spectra were measured in the „reflection" geometry under continuous X-ray excitation (40 kV, 10 mA, tungsten anode). Optical radiation was recorded by MDR-2 monochromator and Hamamatsu H8259-01 photon counting system. The radiation spectrum was measured in the range of 350−650 nm. At the same time a correction was made for the spectral sensitivity of the setup.

Photoluminescence (PL) of films was excited by the 3-rd harmonic radiation of a Nd : YAG-laser (with a wavelength of 355 nm, a repetition frequency of 15 Hz, a pulse duration of ≈ 10 ns) and recorded using a cooled CCD-camera combined with the MDR-206 monochromator. The laser spot size on the samples was about $200\,\mu$m.

XRL kinetics were investigated at pulsed X-ray excitation by the single-photon counting method using the setup described in [14].

All investigations were conducted at a room temperature.

Results and discussion

X-ray diffraction and microscopy studies of samples

According to the results of XRD, samples of ZnO films produced on both the A-plane sapphire and the M-plane sapphire were predominantly [001]-textured (Fig. 1). In addition to the main 002-reflection, 101-reflections and close to them 102- and 103-reflections can be distinguished in XRD patterns of the samples. [103]-oriented crystallites are usually observed in thin ZnO films [13] and in their isostructural nitrides [14]. The presence of their close 102-reflections often can be noted in XRD patterns of (103)-ZnO films [15]. As for inclusions of [101]-crystallites in films, their presence was noted in previous studies as well [16], and their emergence is related to the generation of dislocations at the stage of nucleation. It is worth to note that all reflections of ZnO films were shifted towards the region of greater angles as compared with the standard sample data (JCPDS: 043-0002). In addition, the A-type film has an explicit reflection of substrate (Fig. 1, curve *1*), which is indicative of the smaller thickness of the film.

Thicknesses of samples resulted from the studies of transverse sections by the scanning electron microscopy (SEM) method were significantly different from each other:
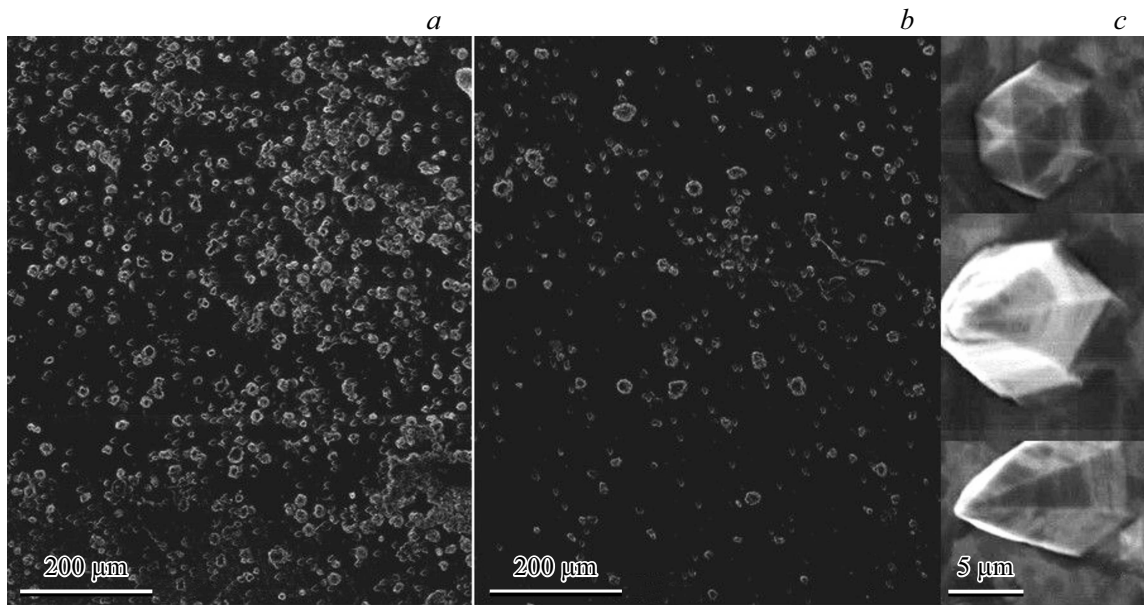
Figure 2. SEM-images of the surface of ZnO films: type M (*a*), type A (*b*). Typical images of [001]-microcrystals of ZnO (*c*).

about $11\,\mu$m for M-type an $6\,\mu$m for A-type. According to the SEM results (Fig. 2), surface of the samples was a continuous layer where explicit [001]-microcrystals of ZnO were formed (Fig. 2, *c*). Lateral size of [001]-microcrystals was as high as $10\,\mu$m. At the same time, in the M-type sample the distribution density of [001]-microcrystals was many times higher than that in the A-type sample (within an area of $100 \times 100\,\mu$m more than 20 microcrystals were observed). Also, in the M-type sample the medium size of microcrystals prevailed.

Based on the obtained results an assumption can be made regarding the model of thick ZnO films growth on M- and A- sapphire. At the initial stage, in accordance with classical concepts of structural-geometric conformity of lattices, films of (103)-ZnO and (001)-ZnO are formed on M- and A- sapphire substrate, respectively. ZnO films are formed in conditions of lack of oxygen in the gaseous phase, therefore the growing films are anion-deficit, with compressed crystalline lattice. This is the cause of the shift of all reflections of the film towards greater angles (decrease in parameters of the lattice cell). The data of XRD (Fig. 1) and SEM (Fig. 2) studies indicate that in the process of growth a transition takes place from the continuous film to nucleation and growth of individual [001]-microcrystals of ZnO. The main condition for the continuous growth of ZnO structure is the excess of zinc in the growth zone. The orientation evolution is connected with the predominance of the normal component of ZnO microcrystals growth with simultaneous decrease in the lateral component of zinc atoms diffusion. In this case, according to the models proposed in [17,18], with decrease in the lateral diffusion component a transition takes place to the columnar structure of the deposit. At a sufficiently high temperature the porous columnar structure can transform

to individual microcrystals. The decrease in the lateral diffusion component of adsorbed atoms (adatoms) is connected with both the roughness of the growth surface of ZnO and the features of magnetron sputtering. It is known that sample in the discharge plasma is subjected to so-called „floating potential" [19]. The dielectric substrate (as well as the growing film) becomes negatively charged, and the ionized positive atoms of zinc, sputtered from the target, receive a component of velocity v_{Zn} towards the substrate. At the same time the diffusion activity along the growing surface decreases and conditions of the transition to nucleation of [001]-microcrystals are implemented. This is confirmed by the transition to growth of individual [001]-microcrystals on the surface of continuous (001)-film of ZnO when the A-substrate sapphire is used. This transition is reflected on the XRD curve as a broadening of the 002-reflection towards greater angles and a decrease in parameter of the cell of ZnO film growing in conditions of zinc excess. The transition from the continuous film of (001)-ZnO to individual [001]-microcrystals of ZnO is hampered, because the energy of homogeneous nucleation is higher than the potential barrier of diffusing adatoms building in the fractures of steps and other defects of the growth surface. Herefrom it follows the low distribution density and small sizes of [001]-microcrystals of ZnO in the A-type film (Fig. 2, *b*). In the case of an M-type sample, due to high surface energy of the (103) plane of ZnO, the transition to [001]-microcrystals takes place at earlier stages. The consequence of the earlier transition is the dense structure and considerably larger sizes of [001]-microcrystals.

Thus, the difference of film thicknesses observed in the SEM-image is connected with the earlier transition to the

growth of individual [001]-microcrystals of ZnO in the M-type sample.

X-ray and photoluminescent properties of samples

Fig. 3 shows XRL spectra of ZnO films on A- and M-sapphire substrates before and after annealing. The radiation spectrum of unannealed films contains a weak near-band-edge luminescence (NBEL) with maxima near 388 and 390 nm for A- and M-type samples, respectively. The XRL intensity of unannealed films is relatively low, which makes it difficult to determine positions of maxima. This may be a consequence of the small thickness. A wide luminescence band in the region of $500-650$ nm (GL) corresponds to the self-defect radiation of ZnO. Small thickness of the film results in that the exposure to radiation also leads to the excitation of substrate material luminescence: some portion of the radiation is in the red range and narrow bands are in the regions of 550, 590, and 620 nm (XRL spectrum of the substrate itself is added in Fig. 3 for comparison). It can be seen, that the radiation intensity of M-type ZnO sample is approximately 2 times higher than that of A-type sample, which may be a consequence of the difference in film thickness, as well as in the distribution density of formed microcrystals.

The annealing resulted in XRL intensity increase of both samples. However, at the same time, different parts of the spectrum have changed differently. Both samples have NBEL intensity grown about 2.5 times (the ratio of intensities remained the same). At the same time, the difference in positions of maximum of NBEL bands has become more explicit. The A-type sample has the intensity maximum at a wavelength of 386 nm, and the M-type sample has it at 388 nm. The GL intensity has grown for both samples as well, however the changes have occurred mainly in the red region of the spectrum. In the green region the intensity of luminescence has grown for the A-type sample only.

For the annealed M-type ZnO film, that had the highest XRL intensity, the XRL kinetics was measured in the time range of $0-20$ ns (Fig. 4). It can be seen, that the main component of the luminescence is in the range of $0-3$ ns and has a decay time (without taking into account the excitation pulse width) of about 0.9-1.1 ns, which corresponds to NBEL of ZnO.

Since the annealing resulted in increased luminescence of films, and in general, samples, especially the M-type film, demonstrate good scintillation properties, in particular, fast XRL decay, studying of their PL-properties was of interest as well. Comparison of PL and XRL spectra contribute to the interpretation of the radiation nature, in particular, the radiation resulted from the X-ray excitation [20].

Fig. 5, a shows PL spectra of annealed films of A- and M- types in UV and visible ranges of wavelengths, that were recorded at an excitation power density of 80 kW/cm². Both spectra demonstrate NBEL bands with maxima at 380.5 and 379 nm in case of A- and M-type films, respectively. Visible
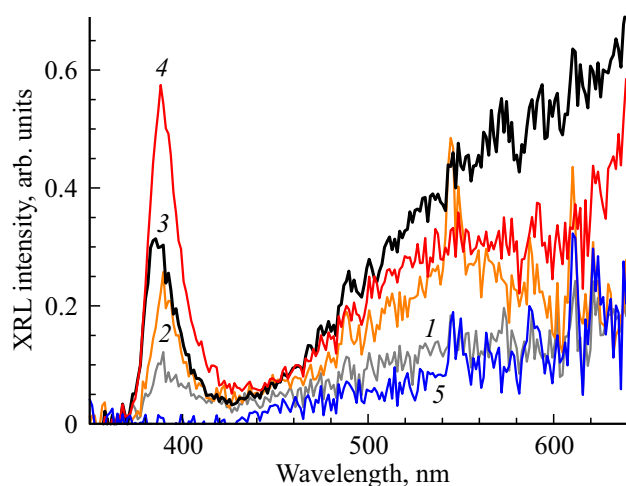

Figure 3. XRL spectra of ZnO films: *1* —unannealed film of A-type, *2* — unannealed film of M-type, *3* — annealed film of A-type, *4* — annealed film of M-type, *5* — sapphire substrate.
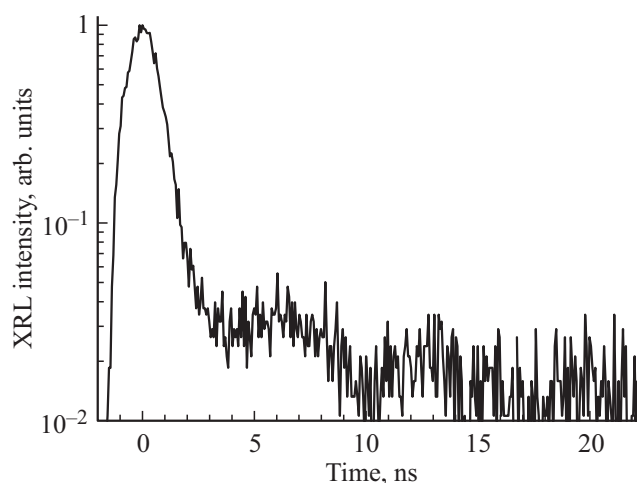

Figure 4. Curve of XRL decay for the M-type ZnO film.

radiation of films was manifested rather weakly as an NBEL shoulder in the range of $420-570$ nm In the spectrum of M-type film and a band in the range of $450-600$ nm in the spectrum of A-type film.

For more detailed NBEL spectra of films, please refer to Fig. 5, b. The NBEL band of both films is composed of several components, in particular, a distinguished long-wave shoulder of the main maximum is observed. In the case of M-type film it is especially explicitly manifested, its maximum corresponds to a wavelength of about 391 nm.

Earlier studies of thin ZnO films produced in similar conditions have shown that the free-carrier concentration in them is $\sim 10^{15}-10^{16}$ cm^{-3} [21]. This results allow expecting the participation of exciton mechanisms in the luminescence of films, provided that relatively low excitation levels are used, such as the Mott threshold is not exceeded yet. Evaluation of the density of electron-hole pairs
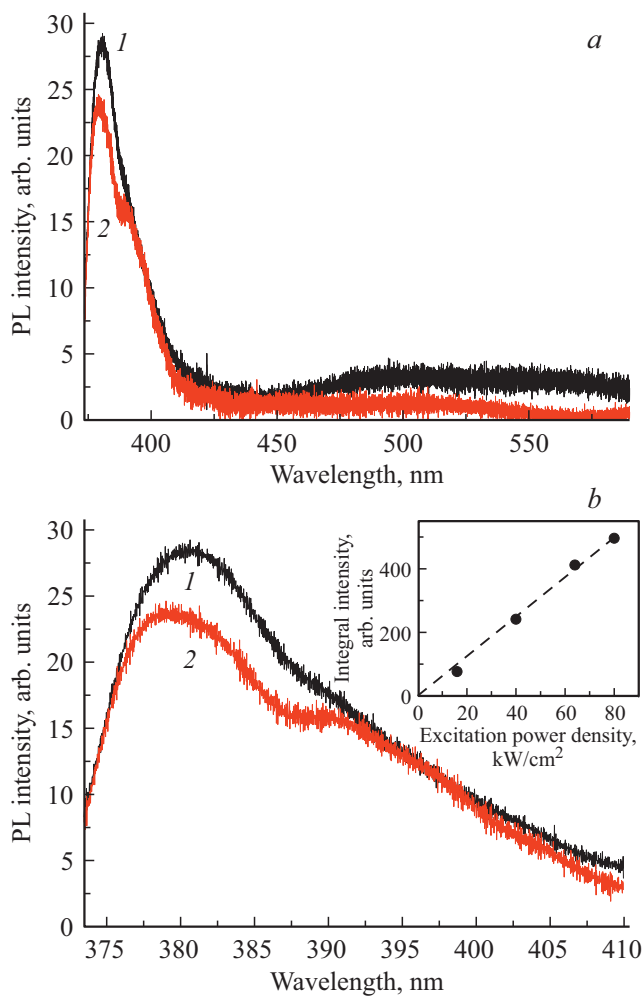
Figure 5. PL spectra of A-type (*1*) and M-type (*2*) films recorded at a power density of $80 \, \text{kW/cm}^2$: (*a*) near UV and partly visible ranges, (*b*) near UV range (EL only). In the insert (*b*) — dependence of integral EL intensity on the photoexcitation level for the M-type film.

Figure 6. EL spectra of annealed A-type (*a*) and M-type (*b*) films recorded at optical (*1*) and X-ray (*2*) types of excitation. Photoexcitation power density is $80 \, \text{kW/cm}^2$. XRL spectra are represented by experimental points and smoothed curves (weighted averaging over neighboring points, 4 points).

generated by the photoexcitation, taking into account their diffusion [20,22,23], yields values not exceeding $10^{17} \, \text{cm}^{-3}$ by the order of magnitude, i.e. not greater than the Mott threshold density for ZnO, which is in the range of $5 \cdot 10^{17} - 4 \cdot 10^{19} \, \text{cm}^{-3}$ according to different sources [23–25].

The dependence of integral NBEL intensity on the level of film excitation measured in the range of $10 - 80 \, \text{kW/cm}^2$ demonstrates a linear behavior (the inset in Fig. 5, *b* shows the dependence for a film of M-type). This behavior is typical for recombination radiation of excitons in contrast to the luminescence, emerging, for example, in case of transitions in donor-acceptor pairs or with participation of a shallow level of defect, where this dependence is often sublinear [26–28].

The quite large NBEL band width (for example, in the case of M-type film the band half-width is $\sim 185 \, \text{meV}$) is indicative of the presence of several radiation channels. In
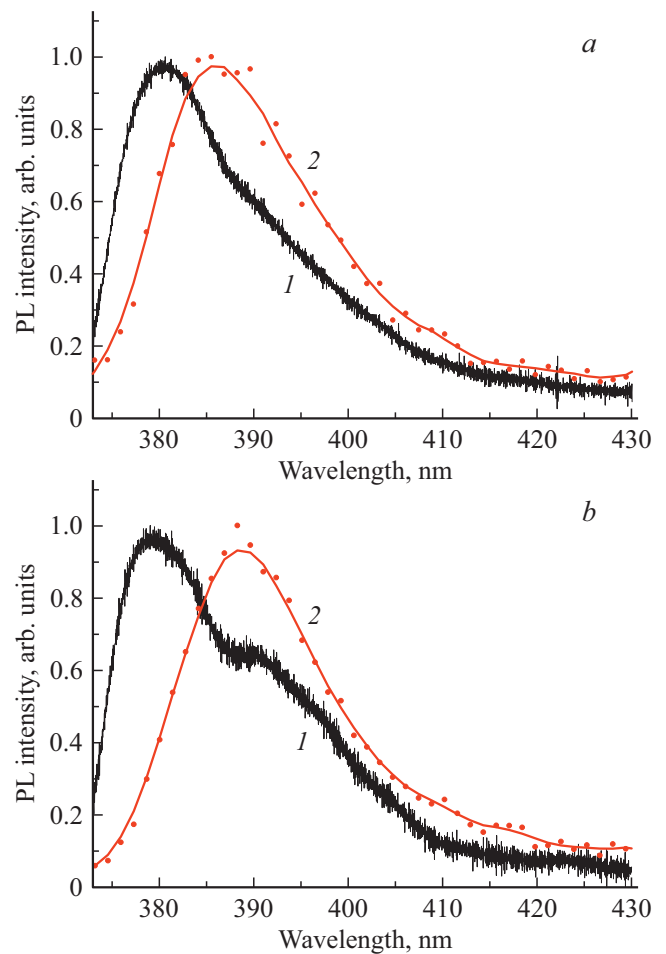
addition to the radiation caused by recombination of free excitons, the participation of its phonon replicas can be assumed (the energy of LO-phonon in ZnO is $72 \, \text{meV}$). The difference between the main maximum ($379 \, \text{nm}$) and its shoulder ($\sim 391 \, \text{nm}$) in the NBEL spectrum of the M-type film is about $100 \, \text{meV}$, and taking into account the overlapping of spectral components, this distance actually is even bigger. This allows making an assumption that the long-wave shoulder is caused mainly by the second phonon replica of the free exciton radiation. It is worth noting that at relatively low excitation power densities in this spectral region in the films and microcrystal structures of ZnO, other types of exciton radiation were reported, in particular, the radiation caused by scattering of excitons on free electrons [29,30]. To clarify the possibility of participation of this and other types of radiation, further investigations are required. In general, the quite high NBEL intensity of the studied films observed at the optical excitation, as well as the explicit exciton charac-

ter of this radiation are indicative of the high samples quality.

Fig. 6 shows comparison between NBEL spectra of annealed films of A-type (Fig. 6, *a*) and M-type (Fig. 6, *b*) recorded at X-ray and optical types of excitation. The spectra are normalized to the maximum, and in the case of XRL, in addition to the experimental spectra shown by dots, smoothed spectra (weighted averaging over neighboring points, 4 points) are shown for ease of comparison. It can be seen that the difference in positions of EL band maxima in XRL and PL spectra is about 6 nm in the case of A-film and 9 nm in the case of M-film, which is comparable with LO-phonon energy in ZnO. In addition, different shapes and widths of NBEL bands at various types of excitation are also observed. In particular, NBEL bands of films in the case of XRL do not contain explicit features connected to the contributions of different types of radiation, as can be observed in PL spectra, which is especially clear seen in the case of M-type film (Fig. 6, *b*).

In case of single-photon excitation, due to the strong absorption of UV light in ZnO (the absorption coefficient for UV photons in ZnO is $\sim (1-2) \cdot 10^5$ cm^{-1} [25]), PL of the films, in contrast to the XRL, is excited in a narrow (up to a few hundreds of nm) near-surface layer. The X-ray quanta penetrate much deeper into the film, to a few micrometers, down to the substrate (see Fig. 3 and comments above). This makes the microfilms different from the case of ZnO structures with nanoscale or submicron crystallites, where the portion of material volume participating in both PL and XRL can be rather high, and, hence, PL and XRL spectra can be similar to each other [7,20]. In the case of microfilm the XRL spectrum in fact reflects the superposition of radiations from the total thickness of the film, being smoothed and hiding the features of radiations from individual layers of the film, including crystallites of different types and orientations. PL spectra at a single-photon excitation are characterized by mainly the same type of microcrystals located in the near-surface layer of the film, and therefore they keep many features of radiation of these microcrystals.

The big difference in positions of NBEL band maximum in case of XRL and PL of films (Fig. 6) probably is connected with the principal contribution to the XRL from the radiation excited in the film body (as compared with the radiation of near-surface regions prevailing in the case of PL). Such radiation, before it leaves the film, travels a significant path within the material, which results in its strong absorption. At the same time, more intensive is absorption of the light with wavelengths closer to the fundamental absorption edge of the material. This results in a relative decrease in the intensity of short-wave edge of the NBEL band and, as a consequence, to a red shift of its maximum.

Conclusion

The results of comparative studies of the processes of high-temperature synthesis, luminescence and scintillation characteristics of ZnO films on M(100)- and A(110)-orientation sapphire substrates are presented. It is shown that the use of the magnetron deposition method makes it possible to form, against the background of a continuous film, ensembles of individual [001] ZnO microcrystals on M(100)- and A(110)-orientation sapphire substrates.

In the case of film on M-sapphire the density of ensemble of [001]-microcrystals of ZnO appeared to be considerably higher and their linear sizes appeared to be bigger than those in the case of film on A-sapphire due to the earlier transition from the growth of continuous film to individual microcrystals. In the XRL spectrum of samples an intensive NBEL band is observed, which was absent when the method of „hot" magnetron sputtering with uncooled target was used. The X-ray luminescence kinetics (NBEL band) is characterized by two components: a fast component with a decay time in the order of a nanosecond and a long shoulder of slow luminescence. The study of the films by photoluminescence spectroscopy revealed the features of the near-band-edge luminescence spectra of the samples, in particular, the presence of various excitonic emission channels. In addition to the recombination radiation of free excitons, an assumption is made regarding significant contribution to the UV radiation of samples from the phonon replicas of free exciton radiation, in particular, the second phonon replica. The quite high NBEL radiation intensity of the studied films observed at the optical excitation, as well as the explicit excitonic character of this radiation confirm high quality of the samples. Comparison of XRL and PL of films allowed identifying their significant differences. In particular, differences are found in the shape of NBEL band and position of its maximum. When interpreting the observed differences, the facts of different depths of UV photons and X-ray quanta penetration into ZnO are taken into account, as well as the absorption of self-radiation of the ZnO in the film.

Thus, the proposed procedure, including depositing with the help of classical magnetron with cooled target and the use of orientation dependence of ZnO structures growth rate is a very promising in the development of scintillation equipment of X-ray range.

Acknowledgments

Funding

Conflict of interest

The authors declare that they have no conflict of interest.

References

[1] B.H. Lin, H.Y. Chen, S.C. Tseng, J.X. Wu, B.Y. Chen, C.Y. Lee, G.C. Yin, S.H. Chang, M.T. Tang, W.F. Hsieh. Appl. Phys. Lett., **109**, 192104 (2016). DOI: 10.1063/1.4967743

[2] B.H. Lin, X.Y. Li, D.J. Lin, B.L. Jian, H.C. Hsu, H.Y. Chen, S.C. Tseng, C.Y. Lee, B.Y. Chen, G.C. Yin, M.Y. Hsu, S.H. Chang, M.T. Tang, W.F. Hsieh. Sci. Rep., **9**, 207 (2019). DOI: 10.1038/s41598-018-36764-8

[3] M.R. Wagner, G. Callsen, J.S. Reparaz, J.H. Schulze, R. Kirste, M. Cobet, I.A. Ostapenko, S. Rodt, C. Nenstiel, M. Kaiser, A. Hoffmann, A.V. Rodina, M.R. Phillips, S. Lautenschläger, S. Eisermann, B.K. Meyer. Phys. Rev. B, **84**, 035313 (2011). DOI: 10.1103/PhysRevB.84.035313

[4] P.A. Rodnyi, K.A. Chernenko, I.D. Venevtsev. Opt. Spectrosc., **125**, 372 (2018). DOI: 10.1134/S0030400X18090205.

[5] K. Oka, H. Shibata, S. Kashiwaya. J. Cryst. Growth., **237** (1), 509 (2002). DOI: 10.1016/S0022-0248(01)01953-4

[6] F. Huang, Z. Lin, W. Lin, J. Zhang, K. Ding, Y. Wang, Q. Zheng, Z. Zhan, F. Yan, D. Chen, P. Lv, X. Wang. Chin. Sci. Bull., **59** (12), 1235 (2014). DOI: 10.1007/s11434-014-0154-4

[7] I.D. Venevtsev, A.P. Tarasov, A.E. Muslimov, E.I. Gorokhova, L.A. Zadorozhnaya, P.A. Rodnyi, V.M. Kanevsky. Materials, **14** (8), 2001, (2021). DOI: 10.3390/ma14082001

[8] I.D. Venevtsev, P.A. Rodnyi, A.E. Muslimov, V.M. Kanevskii, V.A. Babaev, A.M. Ismailov. Opt. Spectrosc., **127**, 1075 (2019). DOI: 10.1134/S0030400X19120282.

[9] A.E. Muslimov, V.M. Kanevsky, I.D. Venevtsev, A.M. Ismailov. Cryst. Rep., **65**, 766 (2020). DOI: 10.1134/S1063774520050144.

[10] K. Tsunekawa. J. Vac. Soc. Japan., **53**, 486 (2010). DOI: 10.3131/jvsj2.53.486

[11] M. Podlogar, J.J. Richardson, D. Vengust, N. Daneu, Z. Samardžija, S. Bernik, A. Rečnik. Adv. Funct. Mater., **22** (15), 3136 (2012). DOI: 10.1002/adfm.201200214

[12] M. Madel, G. Neusser, U. Simon, B. Mizaikoff, K. Thonke. J. Cryst. Growth, **419**, 128 (2015). DOI: 10.1016/j.jcrysgro.2015.03.020

[13] A.E. Muslimov, A.M. Ismailov, Yu.V. Grigoriev, V.M. Kanevsky. J. Surface Investigation: X-ray, Synchrotron and Neutron Techniques., 15, 1195 (2021). DOI: 10.1134/S1027451021060148.

[14] P.A. Rodnyi, S.B. Mikhrin, A.N. Mishin, A.V. Sidorenko. IEEE Trans. Nucl. Sci., **48** (6), 2340 (2001). DOI: 10.1109/23.983264

[15] L. Zhang, J. Wu, T. Han, F. Liu, M. Li, X. Zhu, Q. Zhaoa, T. Yu. Cryst. Eng. Commun., **23** (18), 3364 (2021). DOI: 10.1039/d1ce00040c

[16] E. Chubenko, V. Bondarenko, A. Ghobadi, G. Ulusoy, K. Topalli, A.K. Okyay. MRS Advances, **2** (14), 799 (2017). DOI: 10.1557/adv.2017.150

[17] J. Thornton. Annu. Rev. Mater. Sci., **7**, 239 (1977). DOI: 10.1146/annurev.ms.07.080177.001323

[18] P.B. Barna, M. Adamik. Thin Solid Films., **317**, 27 (1988). DOI: 10.1016/S0040-6090(97)00503-8

[19] A.M. Ismailov, L.L. Emiraslanova, M.K. Rabadanov, M.R. Rabadanov, I.Sh. Aliev. Tech. Phys. Lett., **44**, 528 (2018). DOI: 10.1134/S1063785018060202

[20] A.P. Tarasov, I.D. Venevtsev, A.E. Muslimov, L.A. Zadorozhnaya, P.A. Rodnyi, V.M. Kanevsky. Quantum Electron., **51** (5), 366 (2021). DOI: 10.1070/QEL17534.

[21] A.E. Muslimov, M.Kh. Rabadanov, A.M. Ismailov, Prikladnaya fizika, **3**, 72 (2017) (in Russian).

[22] C.F. Klingshirn. Semiconductor Optics, 4th ed. (Springer, Berlin, 2012).

[23] C. Klingshirn, R. Hauschild, J. Fallert, H. Kalt. Phys. Rev. B, **75**, 1 (2007). DOI: 10.1103/PhysRevB.75.115203

[24] M.A. Versteegh, T. Kuis, H.T.C. Stoof, J. I. Dijkhuis. Phys. Rev. B, **84**, 035207 (2011). DOI: 10.1103/PhysRevB.84.035207

[25] Ü. Özgür, Y.I. Alivov, C. Liu, A. Teke, M. Reshchikov, S. Doğan, V. Avrutin, S.-J. Cho, A.H. Morkoç. J. Appl. Phys., **98**, 11 (2005). DOI: 10.1063/1.1992666

[26] S.A. Studenikin, M. Cocivera. J. Appl. Phys., **91** (8), 5060 (2002). DOI: 10.1063/1.1461890

[27] M.V. Ryzhkov, S.I. Rumyantsev, V.M. Markushev, Ch.M. Briskina, A.P. Tarasov. J. Appl. Spectrosc., **81**, 877 (2014). DOI: 10.1007/s10812-014-0021-8.

[28] S. Rumyantsev, A. Tarasov, C. Briskina, M. Ryzhkov, V. Markushev, A. Lotin. J. Nanophotonics, **10**, 016001 (2016). DOI: 10.1117/1.JNP.10.016001

[29] M. Nakayama, Y. Nakayama. J. Phys. Soc. Japan., **88** (8), 083706 (2019). DOI: 10.7566/JPSJ.88.083706

[30] A.P. Tarasov, L.A. Zadorozhnaya, A.E. Muslimov, Ch.M. Briskina, V.M. Kanevsky. JETP Lett., **114**, 517 (2021). DOI: 10.1134/S0021364021210116.